ISSN 0253-9756 Acta Pharmacol Sin 中国药理学报 2000 Jan; 21 (1): 80 - 86
http://www.simm.ac.cn; www.chinainfo.gov.cn/periodical

Application of secondary structure prediction in antisense drug design targeting protein kinase C-α mRNA and QSAR analysis[1]

SONG Hai-Feng, TANG Zhong-Ming[2], YUAN Shou-Jun, ZHU Bao-Zhen (*Department of Pharmacology, Institute of Radiation Medicine, Academy of Military Medical Sciences, Beijing 100850, China*)

KEY WORDS drug design; antisense oligodeoxyribonucleotides; protein kinase C; secondary protein structure; structure-activity relationship

ABSTRACT

AIM: To optimize the design of antisense drug targeting protein kinase C-α (PKC-α) mRNA and obtain better antisense drugs than ISIS3521 that is undergoing clinical trials. **METHODS**: RNAstructure (version 3.21, 1999) was utilized to predict the optimal and suboptimal secondary structures of human PKCα mRNA (GenBank, X52479), and 29 antisense phosphorothioate oligodeoxynucleotides (S-ODN) targeting the secondary structural elements, 3 partly matched S-ODN and 1 scrambled 3521 were designed. ISIS3521 was set as positive control. Mean ($n = 3 - 5$) 50 % inhibitory effects on proliferation of A549 cells (IC_{50}) of S-ODN were evaluated. Free energies ($\triangle G°_{37}$) relating to the target secondary structural elements were calculated according to the nearest neighbor model. The quantitative structure-activity relationship (QSAR) analysis through multiple regression was obtained by SPSS. **RESULTS**: Three S-ODN: (5′-AGCCCAGCCGCTTGGCTGGG-3′, 5′-AGGAGTGCAGCTGCGTCAAG-3′, 5′-TCAGAGGG-ACTGATGACTTT-3′) had lower IC_{50}[(48 ± 7), (50 ± 4), (64 ± 2.7) nmol·L^{-1}, respectively] than that of ISIS3521 [(81 ± 25) nmol·L^{-1}]. The number of bases comprising the target secondary structural element bulge loop, internal loop, and knot, the free energy of S-ODN ($\triangle G°_{37S}$), and reaction ($\triangle G°_{37R}$) were important parameters in QSAR equation. In the multiple regression, R was 0.68, $P = 0.0193$. Not tally with the equation, two S-ODN (5′-TCAAATGGAGG-CTGCCCGGC-3′, 5′-AAAACGTCAGCCATGGTCCC-3′) with favorable target structures and $\triangle G°_{37}$ did not behave good activities. **CONCLUSION**: Computer aided design was helpful to obtain S-ODN with better *in vitro* effect than current positive drug. The degree of instability of secondary structural elements and $\triangle G°_{37}$ were important factors for drug activity. Other important factors needed for further investigation.

INTRODUCTION

PKC-α, one of classical PKC isoforms, overexpressed in many tumors, and the selected reduction in PKC-α expression caused growth inhibition of tumors or tumor cells[1]. An antisense inhibitor directly against the 3′-untranslated region of PKC-α mRNA, ISIS3521, was already pushed into clinical trials as an anti-neoplasm agent[2]. But according to Eckstein[3], up to now, antisense drugs were screened from S-ODN candidates by random. Then was ISIS3521 the best antisense inhibitor of PKC-α mRNA? To look for better antisense candidates than ISIS3521, we used computer programs RNAstructure to predict the secondary structure of PKC-α mRNA, and then optimized the design of the antisense S-ODN on the basis of the secondary structural elements. The antisense activities *in vitro* on A549 lung cancer cell line of the S-ODN designed were evaluated. Further, QSAR analysis was performed to research the regularity of the antisense drug design.

MATERIALS AND METHODS

Prediction of secondary structures of target mRNA The computer program RNAstructure (ver-

[1] Project supported by the National Natural Science Foundation of China, No 39870877 and the Medicine Hygiene Scientific Research Foundation of PLA, No 98M120.
[2] Correspondence to Prof TANG Zhong-Ming.
Phn 86-10-6693-1230. Fax 86-10-6821-4653.
E-mail tangzm@nic.bmi.ac.cn
Received 1999-08-23 Accepted 1999-10-07

sion 3.21, 1999) was kindly permitted to get, update, and use by Prof Turner DH (Department of Chemistry, University of Rochester, New York 14627) after our registration. The whole human PKC-α mRNA sequence (GenBank entry code: X52479) was obtained from GenBank (available from: URL: http://www.ncbi.nlm.nih.gov/htbin-post/Entrez). The primary sequence was input to the window of RNAstructure, and the parameters were set (maximum energy difference was set at 10 %, maximum number of structures was 20), then RNAstructure calculated the secondary structures of the mRNA based on the principle of minimizing free energy. Finally, the optimal and suboptimal secondary structures of the mRNA would be output.

Calculation of reaction free energy ($\triangle G°_{37R}$) On the basis of the secondary structures with minimum and sub-minimum free energies of PKC-α mRNA predicted by RNAstructure, $\triangle G°_{37}$ was calculated according to the methods of the nearest-neighbor model[4]. All free energy parameters for RNA were in NaCl 1 mol·L^{-1}, at 37 ℃, which were provided in references[5-7]. The $\triangle G°_{37}$ of drug-target-formed duplex ($\triangle G°_{37D}$) was the free energy change associated with duplex formation between the antisense S-ODN and its target sequence. The S-ODN $\triangle G°_{37}$ ($\triangle G°_{37S}$) was the free energy change when the S-ODN formed an internal structure. The target sequence $\triangle G°_{37}$($\triangle G°_{37T}$) was the lowest free energy of the local target mRNA structure. The reaction $\triangle G°_{37}$ ($\triangle G°_{37R}$) was dependent on the $\triangle G°_{37D}$, $\triangle G°_{37S}$, and $\triangle G°_{37T}$ as the formula:

$$\triangle G°_{37R} = \triangle G°_{37D} - \triangle G°_{37S} - \triangle G°_{37T}$$

Design and synthesis of the antisense S-ODN On the basis of the predicted structures of the mRNA, twenty-nine 20-mer S-ODN directly against the local secondary structural element bulge loops, internal loops, hairpins, and knots, which had positive free energies were designed. The anti-PKC-α S-ODN was abbreviated as AP, the number following AP denoted the initiation sites (5′ to 3′ on PKC-α mRNA) of target sequence of the S-ODN, and the number in blankets indicated the length of S-ODN (Tab 1). For example, target sequence of the AP1224 (20) initiated from the 1224th base of the mRNA, and length of the S-ODN was 20-mer. These antisense S-ODN, which bestrewed 5′- and 3′-untranslated region, translated region, initiation codon, and termination codon of the mRNA, were synthesized by Sangon Bioengeneering Company, Shanghai. ISIS3521[8], scrambled 3521, and partly matched S-ODN (APP, Tab 1) were used as positive and negative controls.

Cell culture A549 lung carcinoma cell line (Institute of Materia Medica, Chinese Academy of Medical Sciences) were grown in RPMI-1640 (Gibco, BRL) containing 10 % fetal calf serum (FCS, HyClone) in 37 ℃, 5 % CO_2. The cells were routinely passaged when 85 % – 90 % were confluent.

Treatment of Cells in culture A549 cells were seeded in 96-well plates (NUNC, Denmark) until 50 % – 60 % were confluent (18 – 24 h after passage). At this time, the cells were washed twice with serum-free RPMI-1640, and the S-ODN of required concentration were then transfected into cells by DOTMA/DOPE solution (Lipofectin, Gibco, BRL) according to the instruction of the manufacturer directions. The cells were incubated at 37 ℃ for 6 h, washed twice with RPMI 1640 containing 10 % FCS to remove the Lipofectin, and allowed to recover for an additional 66 h. The thiazolyl blue (MTT, SERVA) solution (0.5 g·L^{-1}) were then added and incubated for another 4 h, then Me_2SO was used to dissolve the precipitation. The absorbance at 570 nm (reference wavelength was set at 450 nm) was determined by Wellscan MK-2 microplate reader (Denley Dragon).

Evaluation of the inhibitory effect on A549 cell proliferation of antisense S-ODN Three to five concentrations (32 – 1000 nmol·L^{-1}) were set to evaluate the antisense activities *in vitro* of every S-ODN and 2 – 4 duplicated wells per concentration were performed. The positive control ISIS3521 was set as working standard on every plate, and each S-ODN was tested for 3 – 5 times in order to obtain reliable results. The concentration *vs* absorbance$_{570\ nm}$ data of each S-ODN were plotted, and 50 % inhibitory concentrations and slopes of S-ODN were calculated using the method of logit analysis by MicroCal Origin software. Mean IC_{50} value ($\bar{x} \pm s$, $n = 3 - 5$ experiments in duplicate) of S-ODN was used as the major criterion of S-ODN inhibitory potency.

QSAR analysis by multiple regression and statistics The IC_{50} value (Tab 1, column 11) was set as dependent variable, and other factors (column 2 – 10) were set as independent variables, then multiple

ISSN 0253-9756 Acta Pharmacol Sin 中国药理学报 2000 Jan; 21 (1)
E-mail aps@server.shcnc.ac.cn Phn/Fax 86-21-6474-2629

regression was executed with the backward elimination method (Criterion POUT = 0.1000), the forward method or the remove method by SPSS (SPSS for windows, computer program. Version 6.0. SPSS Inc; 1993). Statistical inferring was obtained by t test, F test or tests related to the multiple regression performed by SPSS.

RESULTS

Secondary structure of PKC-α mRNA Human PKC-α mRNA was composed of 2245 bases, including 632 adenines (A), 509 uridines (U), 574 guanines (G), and 530 cytosines (C). Five optimal and suboptimal secondary structures with lowest and sub-lowest free energy (−700.3, −697.8, −697.4, −696.2, −695.2 kcal·mol^{-1}) were obtained. In the optimal structure, there were 44 hairpins, 27 bulge loops, 57 internal loops, and 27 knots. These unstable secondary structural elements ($\triangle G°_{37} > 0$) were used as main targets to perform drug design. Twenty-nine antisense S-ODN targeting them and other 4 non-antisense S-ODN [three partly-matched S-ODN: APP1 (20), APP2 (20), APP3 (18), and one scrambled 3521, which have the same base composition with ISIS3521 but a randomized sequence] were designed (Tab 1). Secondary structural elements of target sequences were listed in column 3 to 6 of Tab 1. For instance, target sequence of AP1224 (20) contained a local structure of 2 internal loops and 2 bulge loops. Both of the internal loops were composed of 8 bases (8 +8 in the table), and the two bulge loops were composed of 7 and 3 bases (7+3), respectively (Fig 2). Further, if the local structures of S-ODN were same in all 5 optimal and suboptimal predictions, the stability indicator variable was assigned as 1, otherwise, the variable equals to 0 (Tab 1, column 2).

Calculation of relevant $\triangle G°_{37}$ The 7th, 8th, 9th, and 10th columns in Tab 1 were the results of calculated free energies of S-ODN ($\triangle G°_{37S}$), target mRNA sequence ($\triangle G°_{37T}$), drug-target-formed duplex ($\triangle G°_{37D}$), and reaction ($\triangle G°_{37R}$) (kcal·mol^{-1}). The more negative value of $\triangle G°_{37}$, the higher stability of the S-ODN and the local target structure was implicated, and lower $\triangle G°_{37R}$ meant more possibility to form drug-target duplex, probably a higher biological activity. The results demonstrated that ISIS3521 and all S-ODN tested belonged to the type of possessing low $\triangle G°_{37R}$ and high potential biological activities. On the other hand, partly matched S-ODN and scrambled 3521 had higher $\triangle G°_{37R}$, and their biological activities were supposed poor.

Inhibitory effect on proliferation of A549 cells The inhibitory effect on A549 cells of S-ODN was presented as sigmoid curves, or a linear line on logit-log dose plot. The concentration-effect curve of ISIS3521 was used as reference standard, and a higher potency S-ODN appeared as a line parallel to the curve of standard and shifted to left. On the contrary, the lines of the S-ODN with lower potency shifted to right (Fig 1). The drug effect of the S-ODN could be divided into 5 groups (Tab 1). Among 29 antisense S-ODN designed, three of them [AP1755 (20), AP1224 (20), and AP0973 (20)] had lower IC_{50} than ISIS3521 ($P < 0.01$ for two, $P < 0.05$ for another), and IC_{50} of other 24 antisense S-ODN had no statistical significance compared with ISIS3521. Only 2 individuals [AP1624 (20), AP1768 (20)] had higher IC_{50} than the positive drug ($P < 0.05$). In conclusion, 93 % of the S-ODN designed basing on secondary structure had an inhibitory effect compared with the positive drug that is undergoing clinical trials.

QSAR analysis by multiple regression The variables were set as described in the part of materials and methods. By the backward elimination method of multiple regression in SPSS software, the first eliminated variable was the $\triangle G°_{37D}$, then the variables $\triangle G°_{37T}$ and base number of hairpins in target local structures were orderly removed. At last, 6 independent variables remained in the final equation, and they were the stability indicator variable, base number of bulge loops, internal loops, knots in target local structures, $\triangle G°_{37S}$, and $\triangle G°_{37R}$ (listed in column 2, 3, 4, 6, 7, and 10 of Tab 1). The latter 5 independent variables except the stability indicator had statistically significant T values (Tab 2).

In the end, the most important factors in the QSAR equation were the $\triangle G°_{37R}$ and the number of bases comprising the bulge loops in local target secondary structure. If the multiple regression was performed by the forward method or the remove method in SPSS, the most important variable or the last removed variable was also $\triangle G°_{37R}$ (data not shown).

ISSN 0253-9756 Acta Pharmacol Sin 中国药理学报 2000 Jan; 21 (1)
E-mail aps@server.shcnc.ac.cn Phn/Fax 86-21-6474-2629

Tab 1. Secondary structure, free energy, and inhibitory effect (proliferation of A549 cells *in vitro*) of antisense S-ODN targeting PKC-α mRNA. $n = 3-5$ experiments in duplicate. $\bar{x} \pm s$. (Free energy parameters for RNA were in NaCl 1 mol·L^{-1}, at 37 ℃).

Antisense S-ODN	Structural characteristics of target sequences					Free energy $\triangle G°$ (37 ℃, kcal·mol^{-1})				Inhibitory potency		
	Stability	Bulge loops	Internal loops	Hairpins	Knots	S-ODNs ($\triangle G°_S$)	Targets ($\triangle G°_T$)	Duplexes ($\triangle G°_D$)	Reaction ($\triangle G°_R$)	IC_{50} nmol·L^{-1}	Type	200 nmol·L^{-1} Inhibition %
AP0001 (20)	0	0	8	6	14+14	0.00	−4.65	−41.9	−37.3	97 ± 44	3	78 ± 16
AP0022 (20)	0	0	0	4	14+21	0.00	6.4	−38.6	−45.0	195 ± 140	3	50 ± 41
AP0051 (20)	0	3	0	10	11+21	−2.65	3.2	−42.3	−42.9	94 ± 13	3	77 ± 12
AP0078 (20)	0	0	0	6+8	11	−2.46	−5.6	−39.9	−31.8	117 ± 83	3	70 ± 17
AP0371 (20)	1	0	8+9	0	15	−1.34	−4.75	−39.8	−33.7	92 ± 19	3	65 ± 25
AP0510 (20)	0	0	7	7	11	−2.36	−1.5	−34.1	−30.2	133 ± 35	3	65 ± 22
AP0525 (20)	0	0	7	0	20	−2.11	−1.9	−35.5	−31.5	153 ± 80	3	71 ± 8
AP0658 (20)	1	4	18	0	0	−1.40	−5.1	−34.5	−28.0	101 ± 16	3	76 ± 14
AP0826 (20)	1	3+4	8+6	0	0	−0.18	2.8	−40.4	−43.0	150 ± 51	3	67 ± 15
AP0908 (20)	1	0	8+11+10	0	14	0.00	11.2	−35.6	−46.8	94 ± 28	3	75 ± 14
AP0965 (20)	1	0	0	6	37	−0.88	−3.5	−34.9	−30.5	76 ± 13	2	78 ± 3[b]
AP0973 (20)	1	0	6+9	0	37	−3.96	−7.4	−36.3	−24.9	64.4 ± 2.7[b]	1	79 ± 6[b]
AP1071 (20)	0	0	6	0	24+7	0.00	−4.8	−34.5	−29.7	148 ± 61	3	55 ± 21
AP1184 (20)	1	3	12+8	0	17	−1.53	−4.3	−36.9	−31.1	109 ± 74	3	67 ± 13
AP1224 (20)	1	7+3	8+8	0	0	−2.01	−1.8	−40.5	−36.7	50 ± 4[c]	1	88 ± 6[c]
AP1240 (20)	1	3	8+8	7	0	−3.73	9.4	−40.4	−46.1	114 ± 65	3	71 ± 20
AP1324 (20)	1	0	23+12	0	8	0.00	1.0	−31.1	−32.1	118 ± 26	3	36 ± 12[e]
AP1359 (20)	1	0	9	0	25	−2.27	−6.5	−37.1	−28.3	109 ± 26	3	64 ± 7
AP1380 (20)	1	0	8+6	6	13	−4.33	4.85	−28.2	−28.7	122 ± 47	3	55 ± 25
AP1605 (20)	1	0	23	0	0	0.00	0.1	−31.7	−31.8	118 ± 61	3	61 ± 26
AP1624 (20)	1	3	0	6	14	−1.75	9.2	−41.7	−49.2	399 ± 237[e]	5	27 ± 7[e]
AP1654 (20)	1	0	12+8	0	17	−1.81	0.1	−34.4	−32.7	79 ± 39	2	66 ± 7
AP1738 (20)	1	3	0	0	37	−1.55	−5.2	−38.5	−31.8	126 ± 51	3	69 ± 12
AP1755 (20)	1	3	0	6	0	−12.4	−5.3	−46.1	−28.4	48 ± 7[c]	1	83 ± 11[b]
AP1768 (20)	1	3	0	0	37+14	−3.45	−6.9	−45.5	−35.2	116 ± 25[e]	4	60 ± 17
AP2035 (20)	0	3	0	7	12	−3.49	2.4	−35.4	−34.3	103 ± 37	3	63 ± 23
ISIS3521 (2044)	0	3	0	7	24+12	−1.42	−7.0	−37.0	−28.6	81 ± 25	−	68 ± 10
AP2080 (20)	1	0	13+10	0	0	−3.12	−17.0	−46.9	−26.8	157 ± 78	3	62 ± 11
AP2187 (20)	1	3+3	13+8	0	0	−0.05	0.8	−33.0	−33.8	117 ± 46	3	58 ± 13
AP2209 (20)	1	0	8	13	0	−2.37	−5.4	−33.1	−25.3	139 ± 33	3	52 ± 29
APP1 (20)	0	0	0	0	24	0.00	−	−17.0	−17.0	104 ± 15[e]	4	76 ± 11
APP2 (20)	1	0	23	0	0	−3.05	−	−12.1	−9.05	139 ± 29[e]	4	49 ± 4[f]
APP3 (18)	1	0	0	0	37	0.00	−	−16.6	−16.6	151 ± 35[e]	4	40 ± 7[f]
Scrambled3521	1	0	8	0	0	−2.92	−	−9.60	−6.68	175 ± 52[e]	4	38 ± 20[f]

[b] $P < 0.05$, [c] $P < 0.01$, potency stronger *vs* ISIS3521. [e] $P < 0.05$, [f] $P < 0.01$, potency weaker *vs* ISIS3521.

ISSN 0253-9756 Acta Pharmacol Sin 中国药理学报 2000 Jan; 21 (1)
E-mail aps@server.shcnc.ac.cn Phn/Fax 86-21-6474-2629

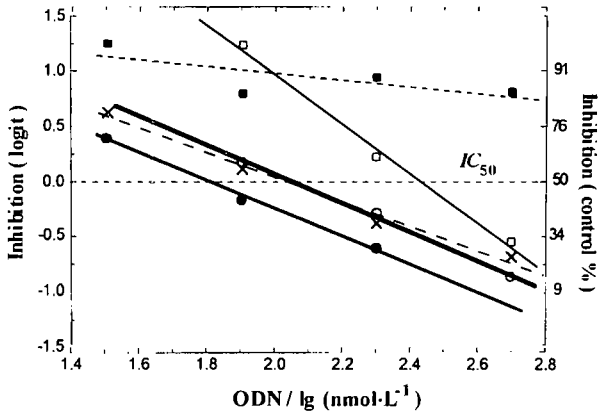

Fig 1. Different inhibitory effects on A549 cells proliferation of the S-ODN. The drug effects of the S-ODN could be divided into 5 groups. ○, positive control ISIS3521; ●, IC_{50} significantly lower *vs* ISIS3521 (group 1), such as AP1224 (20); ×, IC_{50} similar to ISIS3521, including the S-ODN with lower [group 2, such as AP0965 (20)], or higher [group 3, such as AP0525 (20)] IC_{50} *vs* ISIS3521 on numerical values but without statistical significance; □, IC_{50} significantly higher *vs* ISIS3521 (group 4), such as AP1768 (20); ■, almost inefficient S-ODN (group 5), such as AP1624 (20).

DISCUSSION

The core of RNAstructure is an implementation of Zuker algorithm[9,7] to predict RNA secondary structures from sequence based on the principle of minimizing free energy. The thermodynamic data used for these predictions are the latest offered by Turner laboratory[9]. While prediction of RNA secondary structure by free energy minimization will always involve approximations, the structure with lowest free energy may not be the only important structure. Structures with similar free energies may exist in dynamic equilibrium. Equilibria between such structures could be important for function[5]. So the Zuker algorithm was modified for structure prediction to generate suboptimal structures in RNAstructure[9]. In our study, if a local structure was the same in all optimal and suboptimal calculated structures, we considered it is stable and assigned it an indicator variable as 1. Although there is no computer program which can perfectly predict the secondary structure of mRNA, the unceasing consummation of these algorithms and the methods of nucleic acid structure analysis made it possible to improve the accuracy of secondary structure prediction to 82.5 %[10]. The secondary structure-based drug design helped to increase the positive rate.

The calculation of $\triangle G°_{37R}$ based on the secondary structure was helpful for estimating the inhibitory effect of antisense S-ODN. For instance, AP1224 (20), AP0973 (20), and AP1755 (20) had quite low $\triangle G°_{37R}$, and their *in vitro* activities were strong. It was indicated that the reactions between the antisense S-ODN with lower $\triangle G°_{37R}$ and their target sequences might be more inclined to be carried out. However, the computer programs could not supply complete reliability of the secondary structure prediction, needless to say the information of the interrelationships between mRNA and other biomacromolecules such as protein[11]. So some antisense S-ODN we designed did not make our imagination come true. For example, AP1624 (20), AP1768 (20), and AP0022 (20) had favorable $\triangle G°_{37R}$ values and characteristics of local

Tab 2. Variables remained in the equation after the multiple regression with the backward elimination method by SPSS software. $\bar{x} \pm s_{\bar{x}}$.

Variables	B	β	T values	Significance of T
Stability	47 ± 27	0.3583	1.773	0.0895
Base number of bulge loops	−9 ± 4	−0.3856	−2.151	0.0422
Base number of internal loops	−4.6 ± 1.6	−0.7398	−2.919	0.0077
Base number of knots	−1.9 ± 0.9	−0.4650	−2.225	0.0362
$\triangle G°_{37S}$	11 ± 5	0.4350	2.210	0.0374
$\triangle G°_{37R}$	−4.0 ± 1.6	−0.4302	−2.543	0.0182
(Constant)	75 ± 66		1.126	0.2716

Multiple R = 0.68, F = 3.21, P = 0.0193 (n = 29 S-ODN).

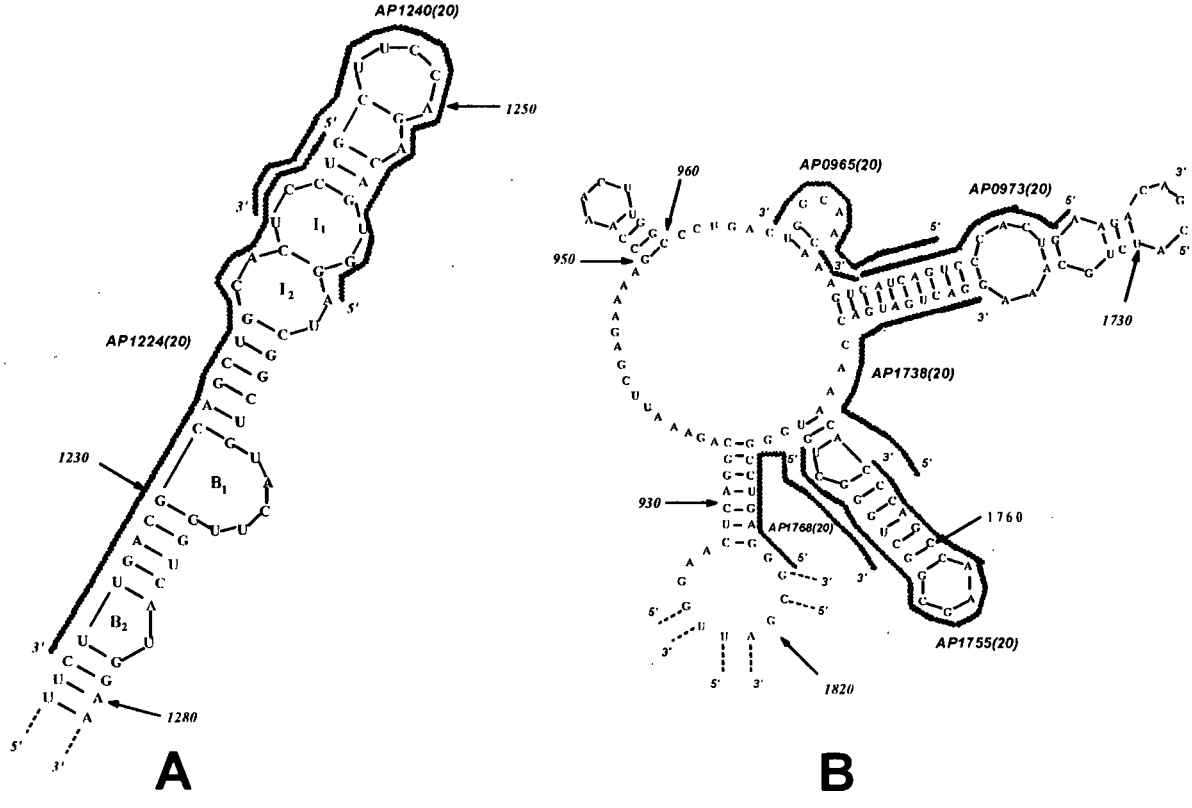

Fig 2. A) Local structure of AP1224 (20) and its target site, including 2 internal loops (I_1, I_2) and 2 bulge loops (B_1, B_2). Another S-ODN with good drug effect, AP1240 (20), located in this local structure too. B) Five S-ODN with acceptable activities including AP1755 (20), AP0965 (20), AP0973 (20) concentrated on this local structure. Two of them were assumed as "motifs".

target secondary structures similar to that with upstanding potency, but their inhibitory effects on proliferation of A549 cells were very poor. It was indicated that a low $\triangle G^{\circ}_{37R}$ was a prerequisite for antisense drug having ideal activity, but many factors other than the $\triangle G^{\circ}_{37R}$ and the internal structures of the target mRNA had influence on the effect of antisense S-ODN. Those factors need for ceaseless struggling research.

The negative controls APP1 (20), APP2 (20), APP3 (18) and scrambled 3521 (Tab 1) were not totally inefficient compared with blank controls. Analysis showed that these S-ODN could also partly match the target mRNA. For example, 12 bases of APP1 (20) could match the bases 2057 – 2068 of PKC-α mRNA, 14 and 9 bases of APP2 (20) and APP3 (18) could match the bases 1607 – 1620 and the bases 946 – 954 of PKC-α mRNA too. Seven bases of the scrambled 3521 could also match target mRNA. This kind of partly-matched bases could also contribute $\triangle G^{\circ}_{37R}$ to a certain extent, so these S-ODN behaved poor inhibitory effect. Probably, this was a kind of "non-sequence-specific antisense effect".

In our study, we found that the antisense S-ODN with high inhibitory effects concentrated on certain regions of the target mRNA, for example, AP1224 (20), AP1240 (20), AP0965 (20), AP0973 (20), etc (Fig 2). It is indicated that there was probably a kind of "motif" in the mRNA structure, which possessed important function and had accessible sites for annealing of antisense S-ODN. If the "motif" could be confirmed by further investigation, the antisense drug design would get twice the result with half the effort. But whether the "motif" do exist and how to determine its position, still need to be studied in the future.

Although S-ODN showed promising inhibitory activities as the first generation antisense oligos, they had certain limitations[12]. In this study, all S-ODN pre-

ISSN 0253-9756 Acta Pharmacol Sin 中国药理学报 2000 Jan; 21 (1)
E-mail aps@server.shcnc.ac.cn Phn/Fax 86-21-6474-2629

sented the "non-specific" cytotoxicity at the concentration as high as 500 nmol·L^{-1}. Other chemical modifications of the ODN[12,13] could not only avoid the non-specific side effects but also help to study the activities and the toxicity of antisense ODN at higher doses. Further, the negative controls were as important as the positive controls[2], more and comprehensive negative controls should be designed and tested in the future studies.

ACKNOWLEDGEMENTS To Prof Turner DH for his support of software and the technical instructions on the usage of the RNAstructure.

REFERENCES

1 Dean N, McKay R, Miraglia L, Howard R, Cooper S, Giddings J, et al. Inhibition of growth of human tumor cell lines in nude mice by an antisense oligonucleotide inhibitor of protein kinase C-α expression. Cancer Res 1996; 56: 3499 - 507.
2 McGraw K, McKay R, Miraglia L, Boggs RT, Pribble JP, Muller M, *et al*. Antisense oligonucleotide inhibitors of isozymes of protein kinase C: *in vitro* and *in vivo* activity, and clinical development as anti-cancer therapeutics. Anti Cancer Drug Design 1997; 12: 315 - 26.
3 Eckstein F. Searching for the ideal partner. Nat Biotechnol 1998; 16: 24.
4 Borer PN, Dengler B, Tinoco IJ, Uhlenbeck OC. Stability of ribonucleic acid double-stranded helices. J Mol Biol 1974; 86: 843 - 53.
5 Turner DH, Sugimoto N, Freier SM. RNA structure prediction. Annu Rev Biophys Biophys Chem 1988; 17: 167 - 92.
6 Freier SM, Kierzek R, Jaeger JA, Sugimoto N, Caruthers MH, Neilson T, *et al*. Improved free-energy parameters for predictions of RNA duplex stability. Proc Natl Acad Sci USA 1986; 83: 9373 - 7.
7 Jaeger JA, Turner DH, Zuker M. Improved predictions of secondary structures for RNA. Proc Natl Acad Sci USA 1989; 86: 7706 - 10.
8 Dean NM, Mckay R, Condon TP, Bennett CF. Inhibition of protein kinase C-α expression in human A549 cells by antisense oligonucleotides inhibits induction of intercellular adhesion molecule 1 (ICAM-1) mRNA by phorbol esters. J Biol Chem 1994; 269: 16416 - 24.
9 Mathews DH, Sabina J, Zuker M, Turner DH. Expanded sequence dependence of thermodynamic parameters improves prediction of RNA secondary structure. J Mol Biol 1999; 288: 911 - 40.
10 Mathews DH, Banerjee AR, Luan DD, Eickbush TH, Turner DH. Secondary structure model of the RNA recognized by the reverse transcriptase from the R2 retrotransposable element. RNA 1997; 3: 1 - 16.
11 Lima WF, Brown-Driver V, Fox M, Hanecak R, Bruice TW. Combinatorial screening and rational optimization for hybridization to folded hepatitis C virus RNA of oligonucleotides with biological antisense activity. J Biol Chem 1997; 272: 626 - 38.
12 Agrawal S, Jiang Z, Zhao Q, Shaw D, Cai Q, Roskey A, *et al*. Mixed-backbone oligonucleotides as second generation antisense oligonucleotides: *in vitro* and *in vivo* studies. Proc Natl Acad Sci USA 1997; 94: 2620 - 5.
13 Temsamani J, Guinot P. Antisense oligonucleotides: a new therapeutic approach. Biotechnol Appl Biochem 1997; 26: 65 - 71.

基于二级结构的靶向蛋白激酶 C-α mRNA 的反义药物设计及构效关系分析[1]

宋海峰，汤仲明[2]，袁守军，朱宝珍
(军事医学科学院放射医学研究所药理研究室，北京 100850，中国)

关键词 药物设计；反义寡脱氧核糖核苷酸类；蛋白激酶 C；二级蛋白质结构；构效关系

目的：通过优化靶向蛋白激酶 C-α mRNA 的反义设计，获得优于阳性药 ISIS3521 的反义药物. **方法**：RNAstructure 预测靶 mRNA 二级结构，针对二级结构单元设计. 体外评价药物对 A549 细胞增殖的抑制效应. SPSS 进行构效关系(QSAR)分析. **结果**：29 个反义药物中 3 个 IC_{50}值显著低于ISIS3521. 靶二级结构单元膨胀环、内环、结点的碱基数、药物结构自由能和反应自由能在 QSAR 方程中有统计意义. 多元回归 $R = 0.68$，$P = 0.0193$. 2 个 S-ODN 有良好的靶结构与自由能但药效差. **结论**：计算机辅助药物设计有助于获得体外药效优于 ISIS3521 的反义药物. 靶二级结构单元的不稳定程度和自由能影响药效. 影响药效的其它因素则有待进一步研究.

(责任编辑 吕 静)